

Study of Lattice Correlation Functions at Small Times using the QCD Sum Rules Continuum Model

Chris Allton¹

*Department of Physics, University of Wales Swansea, Singleton Park,
Swansea SA2 8PP, United Kingdom*

Stefano Capitani²

*DESY - Theory Group, Notkestrasse 85,
D-22607 Hamburg, Germany*

Abstract

In this paper we study the work of Leinweber by applying the Continuum Model of QCD Sum Rules (QCDSR) to the analysis of (quenched) lattice correlation functions. We expand upon his work in several areas: we study meson states as well as baryons; we analyse data from several lattice spacings; and we include data from the Sheikholeslami-Wohlert (clover) improved action. We find that the QCDSR Continuum Model Ansatz can reproduce the data, but only for non-physical values of its parameters. This leads us to reject it as a model for hadronic correlation functions.

We study the non-relativistic quark model and conclude that it predicts essentially the same form for the correlation function as the QCDSR Continuum Model approach. Furthermore, because it doesn't have the Continuum Model's restrictions on the parameters, the non-relativistic quark model can be viewed as a successful Ansatz.

As well as studying the validity or otherwise of the QCDSR Continuum Model approach, this paper defines 4-parameter fitting functions that can be used to fit lattice data even for a time window close to the source. These functions are shown to be an improvement over 2-exponential fits especially in the case of mesons. We encourage the application of this approach to situations where the conventional fitting procedures are problematic due to poor ground state dominance.

¹ E-mail: c.allton@swansea.ac.uk

² E-mail: stefano@mail.desy.de

1 Introduction

Lattice Gauge Theory and QCD Sum Rules (QCDSR) are two areas of research which have been widely employed to deepen the understanding of systems governed by the strong interactions. In this paper we combine both methods following the pioneering work of Leinweber [1,2]. Utilising known results in QCD Sum Rules we apply them to Lattice Gauge Theory in order to check that the two are compatible.

We begin by following the analysis of Refs. [1,2]. In this work, the Continuum Model (often used in QCDSR analyses [3]) is tested using lattice Monte Carlo data. The Continuum Model replaces the discrete spectrum of excited states with a continuum of states of a certain spectral density. This spectral density is calculated using a Wilson OPE expansion of the relevant correlators in the small and intermediate time separation regime. It has been argued that this Continuum Model may be a good approximation to the actual situation of a large set of discrete excited states [3,1].

We extend the work of Refs. [1,2] by including mesonic states. We also apply our analysis to several β values (corresponding to different lattice spacings), and to two actions with different lattice artefacts (namely the Wilson action [4] and the “clover” Sheikholeslami-Wohlert (SW) improved action [5]). Thus we are able to study the effects of lattice artefacts in the calculation. The lattice data we use in this study is from the APE Collaboration. As in the analysis of [1], we use zero-momentum correlation functions. At first sight the analysis suggests that the QCDSR Continuum Model is in reasonably good agreement with the lattice data, confirming the results of [1]. However, this agreement is ambiguous since we also find that the naive (non-relativistic) quark model predicts essentially the same behaviour as the Continuum Model. Furthermore, because we have data at different lattice spacings, we are able to test the continuum scaling behaviour. We find that the parameter introduced to take account of lattice distortions in the Continuum Model does not scale towards its predicted value as the lattice spacing is reduced. Thus we conclude from our analysis that there are reservations regarding the validity of the QCDSR Continuum Model (but confirmation of the quark model). We also test the relativistic quark model against our data and find poorer agreement.

Through this study of the QCDSR Continuum Model, we have defined a procedure which enables lattice correlation functions to be fitted at small (Euclidean) time values. This can be usefully employed in the case of correlation functions that have numerical problems in the isolation of the ground state properties at large time separations. By fitting the lattice correlation function data to a term

representing the ground state contribution, plus a term representing the contributions of the excited states, we show that accurate ground state parameters can be extracted even when the fitting window is very close to the source. We explicitly show that these QCDSR-inspired fitting functions reproduce the parameters of the ground state better than the conventional, double-exponential fitting procedure.

Recently, some other researchers have also used Continuum Model ideas to study lattice correlation functions [6,7]. They study hadronic correlation function, but use configuration space (i.e. point-to-point functions; see also [8]) rather than the momentum space correlation functions analysed here.

This paper is organised as follows: in Sect. 2 details of the lattice data used in our analysis are given; Sect. 3 describes the QCD Sum Rules approach; in Sect. 4 results are presented for these fits; in Sect. 5 we present results using the quark model; and finally, in Sect. 6 there is a discussion and conclusion. An earlier version of this work appeared in [9].

2 Lattice Details

The lattice data used in this study is from the APE collaboration and uses the quenched approximation. Specifically it is data which has been used primarily in the study of weak matrix elements such as f_B and B_K [10–12], and, more recently, for light hadronic spectroscopy [13]. A list of the simulation parameters is presented in Table 1. For full details of the simulations, see the corresponding reference. All errors in the results were obtained using the Jackknife method with 10 configurations eliminated per cluster.

The lattices in this study span a range of β -values which correspond to different lattice spacings, a . In Table 1 and throughout this paper, a is set from the K and K^* masses following the approach described in [13]. This method avoids any chiral extrapolation and uses data at the simulated values of the quark masses, i.e. at around the strange mass. It is therefore preferable than other methods, e.g. obtaining a^{-1} from the ρ -mass etc. Note that the lattice spacings are smaller than those used in Refs. [1] and [2] and so clearly lattice artefacts should be smaller.

Typically each simulation was performed with three different values of the hopping parameter, κ . Only one of these (for each simulation) was chosen to be included in this study. This choice was made so that the vector meson masses in physical units from each simulation were equal to 1.1 GeV within errors (see Table 1). The one exception to this is the Wilson case at $\beta = 6.1$ where there

Table 1

Simulation parameters used. The inverse lattice spacing a^{-1} was obtained from the K and K^ masses [13].*

Ref.	β	Action	Number of Configs	Lattice Volume	a^{-1} [GeV]	a [fm]	κ	M_V [GeV]
[11]	6.0	Clover	200	$18^3 \times 64$	2.01(6)	0.098(3)	0.1425	1.10(3)
[10]	6.2	Clover	200	$18^3 \times 64$	3.0(3)	0.065(6)	0.14144	1.14(11)
[11]	6.4	Clover	400	$24^3 \times 64$	3.9(2)	0.050(2)	0.1403	1.12(4)
[12]	6.0	Wilson	200	$18^3 \times 64$	2.27(4)	0.087(2)	0.1530	1.11(2)
[11]	6.1	Wilson	230	$18^3 \times 64$	2.7(2)	0.073(4)	0.1510	1.27(8)
[11]	6.4	Wilson	400	$24^3 \times 64$	4.1(2)	0.048(2)	0.1492	1.10(3)

was no κ value available to match this requirement.

The (zero-momentum) hadronic correlation function is defined for mesons as

$$G_2(t) \equiv \sum_{\vec{x}} \langle 0 | T \{ J(\vec{x}, t) \bar{J}(\vec{0}, 0) \} | 0 \rangle. \quad (1)$$

While the definition of the meson correlators is standard, the definition of the nucleon and delta correlation functions is specific to the APE simulations, and is given by

$$G_2(t) \equiv \sum_{\vec{x}} \text{tr} \left[\frac{1 + \gamma_4}{4} \langle 0 | T \{ J(\vec{x}, t) \bar{J}(\vec{0}, 0) \} | 0 \rangle \right], \quad (2)$$

where the projector $(1 + \gamma_4)$ onto positive parity states is introduced. Another common definition for the nucleon correlation function is the one used by the UKQCD Collaboration (see for example [7,14]). It is given by

$$G_2(t) \equiv \sum_{\vec{x}} \text{tr} \left[\frac{1}{4} \langle 0 | T \{ J(\vec{x}, t) \bar{J}(\vec{0}, 0) \} \gamma_\mu x_\mu | 0 \rangle \right]. \quad (3)$$

Of specific interest to this work is the definitions of the interpolating operators, J , defined below. The channels analysed in this work are the nucleon, pseudoscalar meson, (spatial component of the) vector meson and (temporal component of the) axial meson. The other channels are included below for completeness.

Nucleon:

$$J(\vec{x}, t) = \sum_{\delta} [u^a(\vec{x}, t) \mathcal{C} \gamma_5 d^b(\vec{x}, t)] u_{\delta}^c(\vec{x}, t) \epsilon_{abc} \quad (4)$$

Delta: see [15]

$$J(\vec{x}, t) = \sum_{\mu=2}^3 \sum_{\delta} [u^a(\vec{x}, t) \mathcal{C} \gamma_{\mu} u^b(\vec{x}, t)] u_{\delta}^c(\vec{x}, t) \epsilon_{abc} \quad (5)$$

Scalar meson:

$$J(\vec{x}, t) = \bar{u}^a(\vec{x}, t) d^a(\vec{x}, t) \quad (6)$$

Pseudoscalar meson:

$$J(\vec{x}, t) = \bar{u}^a(\vec{x}, t) \gamma_5 d^a(\vec{x}, t) \quad (7)$$

Vector meson (spatial components):

$$J(\vec{x}, t) = \frac{1}{3} \sum_i \bar{u}^a(\vec{x}, t) \gamma_i d^a(\vec{x}, t) \quad (8)$$

Vector meson (temporal component):

$$J(\vec{x}, t) = \bar{u}^a(\vec{x}, t) \gamma_4 d^a(\vec{x}, t) \quad (9)$$

Axial meson (spatial components):

$$J(\vec{x}, t) = \frac{1}{3} \sum_i \bar{u}^a(\vec{x}, t) \gamma_5 \gamma_i d^a(\vec{x}, t) \quad (10)$$

Axial meson (temporal component):

$$J(\vec{x}, t) = \bar{u}^a(\vec{x}, t) \gamma_5 \gamma_4 d^a(\vec{x}, t). \quad (11)$$

In these equations, the indices a, b, c refer to colour, δ is a spinorial index and $\mathcal{C} = \gamma_4 \gamma_2$ is the charge conjugation matrix.

All the baryonic correlation functions presented in this work have the sum over \vec{x} in Eq. (2) replaced by a sum over every 3rd lattice site in each of the three spatial directions. This procedure, called “thinning”, is due to the limitations imposed on the calculation by the size of the APE memory. It introduces extra states in the correlation functions which are not present when the usual full sum over \vec{x} is taken. These unwanted states have large energy corresponding to large spatial momenta and do not affect the conventional extraction of the ground state

properties [16,10,13]. This is because at the (relatively large) times where there is ground state dominance, the higher energy states have decayed away. However, since the procedure presented in this paper uses small time values, thinning does have an effect which will be referred to in Sect.4.3.

3 QCD (Sum Rules) Continuum Model

In this section we describe the QCDSR Continuum Model. The basic object in this approach is the quark propagator in Euclidean space whose first few polynomial terms in the Wilson OPE expansion read [1,6] (in the coordinate gauge, $x^\mu A_\mu = 0$),

$$S_q^{aa'} = \frac{1}{2\pi^2} \frac{\gamma \cdot x}{x^4} \delta^{aa'} + \frac{1}{4\pi^2} \frac{m_q}{x^2} \delta^{aa'} - \frac{1}{8\pi^2} \frac{m_q^2}{x^2} \frac{\gamma \cdot x}{x^2} \delta^{aa'} - \frac{1}{2^2 3} \langle : \bar{q} q : \rangle \delta^{aa'} + \dots \quad (12)$$

From Eqs. (1,2 & 3), the timesliced (three-momentum-projected) two-point correlation function then has the OPE expansion

$$G_2^{OPE}(t) = \sum_{n=-\infty}^{n_0} \frac{1}{t^n} \cdot C_n O_n(m_q, \langle : \bar{q} q : \rangle), \quad (13)$$

where C_n is a numerical coefficient, O_n is some function, and n_0 a positive integer. For the nucleon and delta, this leading term turns out to be $n_0 = 6$ for the APE definition Eqs. (2). However, different definitions of the correlators lead to different QCDSR Continuum Model formulae, and if we were to use the UKQCD definition, Eq. (3), we would have $n_0 = 5$ for both the nucleon and delta. For the mesons the exponents of the leading terms are given by $n_0 \leq 3$.

It is now useful to express the timesliced correlation function, $G_2(t)$, in the spectral representation

$$G_2(t) = \int_0^\infty \rho(s) e^{-st} ds. \quad (14)$$

The OPE expansion of the spectral density function, $\rho^{OPE}(s)$, is calculated by means of a simple inverse Laplace transform of Eq. (13),

$$\rho^{OPE}(s) = \sum_{n=1}^{n_0} \frac{s^{n-1}}{(n-1)!} \cdot C_n O_n(m_q, \langle : \bar{q} q : \rangle), \quad (15)$$

where $Re(t) > 0$. In the sum over n , we have kept only the positive values of n since we are interested in the leading terms as $t \rightarrow 0$.

The QCD Continuum Model is introduced at this stage by setting a threshold s_0 in the energy scale s in Eq. (14), so that the excited states' contribution to $G_2(t)$ is given only by the energies above s_0 . Performing the integral over s we obtain,

$$\begin{aligned} G_2^{cont}(t) &\equiv \int_{s_0}^{\infty} \rho^{OPE}(s) e^{-st} ds \\ &= e^{-s_0 t} \sum_{n=1}^{n_0} \sum_{k=0}^{n-1} \frac{1}{k!} \frac{s_0^k}{t^{n-k}} \cdot C_n O_n(m_q, \langle : \bar{q} q : \rangle). \end{aligned} \quad (16)$$

Thus the continuum contribution to the correlation function has been derived using QCDSR style considerations. The hope is that it correctly models the discrete states in the spectrum above the ground state.

However, the full correlation function contains the ground state as well as the above continuum contribution G_2^{cont} . In the quenched approximation, the ground state contributes a delta function to the full spectral density [1,7]:

$$\rho(s) = \frac{Z}{2M} \delta(s - M) + \theta(s - s_0) \rho^{OPE}(s) \quad (17)$$

where $\rho^{OPE}(s)$ is given by Eq. (15). The full correlation function can then be written as (from Eqs. (14 & 16))

$$\begin{aligned} G_2(t) &= \frac{Z}{2M} e^{-Mt} + \xi \int_{s_0}^{\infty} \rho^{OPE}(s) e^{-st} ds \\ &= \frac{Z}{2M} e^{-Mt} + \xi e^{-s_0 t} \sum_{n=1}^{n_0} \sum_{k=0}^{n-1} \frac{1}{k!} \frac{s_0^k}{t^{n-k}} \cdot C_n O_n(m_q, \langle : \bar{q} q : \rangle) \end{aligned} \quad (18)$$

There are four parameters in this Ansatz for $G_2(t)$:

- Z is the normalization of the ground state. Note that in [1,2] the parameter λ_1 was used. λ_1 and Z are related by $\lambda_1^2 = Z/(2M)$;
- M is the mass of the ground state particle;
- ξ is a new parameter introduced to normalise the contribution of the excited states [1]. In the continuum limit, ξ should be equal to one. (We will discuss this in more detail in Sect. 4.3);
- s_0 is the continuum threshold which parametrises the onset of the excited states.

We have developed some FORM codes able to calculate the coefficients C_n in the expansions in Eqs. (13) and (18) for the operators in Eqs. (4 - 11). The relevant OPE expansions (i.e. the $G_2^{OPE}(t)$ in Eq. (13)) turn out to be:

Nucleon (APE data):

$$G_2^{OPE}(t) = \frac{75}{256\pi^4} \frac{1}{t^6} + \frac{21}{64\pi^4} \frac{m_q}{t^5} - \frac{3}{16\pi^4} \frac{m_q^2}{t^4} - \frac{7}{32\pi^2} \frac{\langle : \bar{q}q : \rangle}{t^3} + \dots \quad (19)$$

Delta (APE data):

$$G_2^{OPE}(t) = \frac{45}{32\pi^4} \frac{1}{t^6} + \frac{15}{8\pi^4} \frac{m_q}{t^5} - \frac{15}{4\pi^2} \frac{\langle : \bar{q}q : \rangle}{t^3} + \dots \quad (20)$$

Scalar meson:

$$G_2^{OPE}(t) = \frac{3}{4\pi^2} \frac{1}{t^3} - \frac{9}{4\pi^2} \frac{m_q^2}{t} + \dots \quad (21)$$

Pseudoscalar meson:

$$G_2^{OPE}(t) = -\frac{3}{4\pi^2} \frac{1}{t^3} + \frac{3}{4\pi^2} \frac{m_q^2}{t} + \dots \quad (22)$$

Vector meson (Spatial components):

$$G_2^{OPE}(t) = -\frac{1}{2\pi^2} \frac{1}{t^3} + \dots \quad (23)$$

Axial meson (Temporal components):

$$G_2^{OPE}(t) = \frac{-3}{2\pi^2} \frac{m_q^2}{t} + \dots \quad (24)$$

Axial meson (Spatial components):

$$G_2^{OPE}(t) = \frac{1}{2\pi^2} \frac{1}{t^3} - \frac{3}{2\pi^2} \frac{m_q^2}{t} + \dots \quad (25)$$

Note that for the vector meson, the leading term for the temporal component is $\mathcal{O}(m_q^4)$. Since this corresponds to the first *neglected* term in the OPE expansion for the quark propagator in eq.(12), it is beyond the scope of this work and we therefore do not consider this channel again. Note also that there is no term $\mathcal{O}(m_q^2)$ for the spatial component of the vector correlation function.

In the nucleon and delta case we have included for completeness the contribution of the vacuum condensate. However, in practice, it is not necessary to consider neither this term nor the m_q^3/t^3 term, since they are numerically irrelevant. We note that Leinweber came to the same conclusion [1]. It is important to note that for all mesons listed there is no term appearing which is one order in t smaller than the leading term. i.e. the first nonzero correction, with respect to the leading term, is of order t^2 and not t as we would naively expect. Similarly, the order t^3 term (with respect to the leading term) is zero. The first appearance of the vacuum condensate $\langle : \bar{q}q : \rangle$ in the meson case is of order t^4 relative to the leading term, rendering its contribution totally insignificant.

We give here for the sake of completeness the correlation functions corresponding to Eq. (18), i.e. the $G_2(t)$ actually used to fit the lattice data. They are:

Nucleon (APE data):

$$\begin{aligned} G_2(t) = & \frac{Z}{2M} e^{-Mt} \\ & + \xi e^{-s_0 t} \cdot \left[\frac{75}{256\pi^4} \left(\frac{1}{t^6} + \frac{s_0}{t^5} + \frac{1}{2} \frac{s_0^2}{t^4} + \frac{1}{6} \frac{s_0^3}{t^3} + \frac{1}{24} \frac{s_0^4}{t^2} + \frac{1}{120} \frac{s_0^5}{t} \right) \right. \\ & + \frac{21}{64\pi^4} m_q \left(\frac{1}{t^5} + \frac{s_0}{t^4} + \frac{1}{2} \frac{s_0^2}{t^3} + \frac{1}{6} \frac{s_0^3}{t^2} + \frac{1}{24} \frac{s_0^4}{t} \right) \\ & \left. - \frac{3}{16\pi^4} m_q^2 \left(\frac{1}{t^4} + \frac{s_0}{t^3} + \frac{1}{2} \frac{s_0^2}{t^2} + \frac{1}{6} \frac{s_0^3}{t} \right) \right] \quad (26) \end{aligned}$$

Delta (APE data):

$$\begin{aligned} G_2(t) = & \frac{Z}{2M} e^{-Mt} \\ & + \xi e^{-s_0 t} \cdot \left[\frac{45}{32\pi^4} \left(\frac{1}{t^6} + \frac{s_0}{t^5} + \frac{1}{2} \frac{s_0^2}{t^4} + \frac{1}{6} \frac{s_0^3}{t^3} + \frac{1}{24} \frac{s_0^4}{t^2} + \frac{1}{120} \frac{s_0^5}{t} \right) \right. \\ & \left. + \frac{15}{8\pi^4} m_q \left(\frac{1}{t^5} + \frac{s_0}{t^4} + \frac{1}{2} \frac{s_0^2}{t^3} + \frac{1}{6} \frac{s_0^3}{t^2} + \frac{1}{24} \frac{s_0^4}{t} \right) \right] \end{aligned}$$

Scalar mesons:

$$G_2(t) = \frac{Z}{2M} e^{-Mt} + \xi e^{-s_0 t} \cdot \left[\frac{3}{4\pi^2} \left(\frac{1}{t^3} + \frac{s_0}{t^2} + \frac{1}{2} \frac{s_0^2}{t} \right) - \frac{9}{4\pi^2} \frac{m_q^2}{t} \right] \quad (27)$$

Pseudoscalar mesons:

$$G_2(t) = \frac{Z}{2M} e^{-Mt} - \xi e^{-s_0 t} \cdot \left[\frac{3}{4\pi^2} \left(\frac{1}{t^3} + \frac{s_0}{t^2} + \frac{1}{2} \frac{s_0^2}{t} \right) - \frac{3}{4\pi^2} \frac{m_q^2}{t} \right] \quad (28)$$

Vector mesons (Spatial components):

$$G_2(t) = \frac{Z}{2M} e^{-Mt} - \xi e^{-s_0 t} \cdot \left[\frac{1}{2\pi^2} \left(\frac{1}{t^3} + \frac{s_0}{t^2} + \frac{1}{2} \frac{s_0^2}{t} \right) \right] \quad (29)$$

Axial mesons (Temporal components):

$$G_2(t) = \frac{Z}{2M} e^{-Mt} - \xi e^{-s_0 t} \cdot \left[\frac{3}{2\pi^2} \frac{m_q^2}{t} \right]. \quad (30)$$

Axial mesons (Spatial components):

$$G_2(t) = \frac{Z}{2M} e^{-Mt} + \xi e^{-s_0 t} \cdot \left[\frac{1}{2\pi^2} \left(\frac{1}{t^3} + \frac{s_0}{t^2} + \frac{1}{2} \frac{s_0^2}{t} \right) - \frac{3}{2\pi^2} \frac{m_q^2}{t} \right]. \quad (31)$$

We have carried out several four-parameter fits to the nucleon, pseudoscalar, vector (spatial components) and axial-vector (temporal components) using Eqs. (26, 28, 29 & 30) to check the ideas presented in this paper. The results of these fits are described in detail in the following Section.

One could also introduce a further parameter Λ as upper limit of integration over s in Eq. (18) to account for the lattice cut-off. Ref. [1] reports that this does not make any difference as long as t is not taken less than two. For this reason we restrict our fits to $t \geq 2$.

4 Fits to data

Correlation functions from the simulations outlined in table 1 were fitted to the following three different functional forms:

Conventional Single State Fit (“1-exp”)

$$F(t) = \frac{Z}{2M} e^{-Mt} \quad (32)$$

This is the usual functional form used in the study of lattice correlation functions.

QCD Continuum Model Fit (“*Cont*”)

The fitting forms in Eqs. (26-31). (i.e. those obtained from the O.P.E. plus the Continuum Model assumption in Sect. 3)

Conventional Two State Fit (“*2-exp*”)

$$F(t) = \frac{Z}{2M}e^{-Mt} + \frac{Z'}{2M'}e^{-M't} \quad (33)$$

This functional form was chosen since it is traditionally used as the generalisation of Eq. (32) when attempts are made to include the effects of the higher mass state(s). It is an alternative to the Continuum Model fits (i.e. it has the same number of parameters) and the results of both fits will be directly compared.

Note that for the mesons, we have symmetrised the ground state exponential in time for all three cases above by taking into account the backward moving state in the fits.

The conventional single state fits are only valid for asymptotic states. This limits their applicability to a time window where the “effective mass” is constant in time.³ We use the results of these fits (in the asymptotic region) as standard values of the ground state fitting parameters Z and M with which to compare the results of the other two fitting methods. A list of the parameters Z and M and the χ^2 obtained from these single state fits, is displayed in Tables 2,3,4 & 5 in the rows marked “*1-exp*”. The four channels: nucleon and the pseudoscalar, vector (spatial components) and axial (temporal component) mesons were analysed.

The time windows used in each of the fitting methods are listed in Table 6 and are chosen so that the effective masses are stable. The starting points in the windows are a function of the β value, as expected, since the lattice spacing varies with β . In the case of the QCD Continuum Model fits, we use time windows which begin very close to the origin: $t = 2 - 28$ for $\beta = 6.0$; $t = 3 - 28$ for $\beta = 6.1$ & 6.2 ; $t = 4 - 28$ for $\beta = 6.4$. (See Table 6.) The starting times for these windows are chosen with the criterion that $t \geq 2$ (see Sect. 3) and that they are approximately equal in physical units for all simulations. The results of these fits are displayed in Tables 2,3,4 & 5 in the rows marked “*Cont*”.

So that a direct comparison can be performed, the same time windows were used to perform conventional two state fits using Eq. (33). The results of the fitting parameters from these fits are also displayed in Tables 2,3, 4 & 5 in the rows

³ The effective mass is defined as $\log(G_2(t)/G_2(t+1))$.

labelled “2-exp”.

We now discuss the results of these fitting methods in detail.

4.1 Ground State Parameters

Concentrating on the comparison of the ground state parameters, Z and M , from the “Cont” fit with those from the “1-exp” fit, we see good agreement for the mesonic states. This is particularly encouraging because very small time values were included in the fitting window.⁴ However, for the baryons, poorer agreement is observed. In fact the agreement between the Z and M values from the Continuum Model and “1-exp” fit becomes worse as β increases (i.e. as the continuum limit is approached). Overall, these fits suggest that the QCD Continuum Model is a reliable method of extracting ground state information in the mesonic case, but that there is some question about its validity for the baryons. Note that Leinweber, who studied baryons only, found good agreement [1]. A possible explanation for this is that he used data at a larger lattice spacing and with poorer statistics than those studied here. Note also that the baryonic data is “thinned” which will obviously affect the normalisation of the higher mass states. This could conceivably also affect the ground state fitting parameters in the “Cont” fits.

The results for Z and M for the “2-exp” fits require careful interpretation. Comparing the “2-exp” and “1-exp” fits we see that the values for both Z and M for the “2-exp” fits are larger than those in the “1-exp” fit *in every case*. This presumably means that the introduction of a “raw” second exponential biases the parameters of the asymptotic state. Also, it can be seen that in every case except one (the Wilson $\beta = 6.0$, Pseudoscalar meson) the “Cont” values for Z and M reproduce the “standard values” (i.e. the “1-exp” values) better than the “2-exp” do.

We can understand this bias in the case of the “2-exp” fit as follows. The true set of states that contributes to the spectrum includes the ground state and many excited states. In the case of the “2-exp” fit, all the excited states are modelled as a single state. Clearly the values of M' and Z' from this fit will be some average over all the excited states. This means that the M' value will be larger than the *first* excited state’s mass. However, of the excited states, it is this first excited state that is the most significant correction to the ground state at intermediate values of t (i.e. at t values large enough so that the excited states are no longer dominant, and small enough so that the ground state also has not yet dominated

⁴Note also that it is well known that the statistical errors in the fitted Z and M values typically underestimate the real errors due to correlations in the data [17].

the correlation function). This means that the correlation function for the “2-exp” fit will be too small in these intermediate values of t . To adjust for this mismatch, the value of the ground state’s mass, M (and Z since they are correlated) will be shifted slightly higher in the “2-exp” fit.

Obviously, in order to avoid this bias, correct account must be taken of all the excited states in the spectrum. The Continuum Model is one way of modelling these states, and thus should overcome at least part of the above shortcomings of the “2-exp” fit. The agreement of the ground state parameters, Z and M , between the Continuum Model and “1-exp” fit confirms this hypothesis.

4.2 *Quality of the Fits*

Turning to the χ^2 values, the first thing to note is that the $\chi^2/\text{d.o.f.}$ for the “Cont” and “2-exp” fits can be as much as 10 or 100. At first sight this is a worrying feature, especially since the χ^2 is calculated ignoring correlations between timeslices. (The presence of correlations canonically lowers the uncorrelated $\chi^2/\text{d.o.f.}$ to below unity.) However, the correlation function data at small times has relatively tiny errors compared with large times. (Typically the correlation function has statistical errors of one part in a thousand at the beginning of the fitting window, and around one part in ten at the end of the window.) Therefore any small discrepancy between the fitting functions and the data at small times leads to a very large contribution in the χ^2 . It is unreasonable to expect that the small time behaviour of the correlation functions could possibly be reproduced *at the level of these tiny statistics* by any model containing only four parameters, no matter how well physically motivated. It is also worth bearing in mind that the meson correlation functions fall by from 3 to as much as 7 orders of magnitude in the region fitted in the “Cont” and “2-exp” cases. In the case of the baryons the correlation functions can fall by as much as 13 orders of magnitude. Fig. 1 shows the (natural) logarithm of the correlation function for the vector meson in the Wilson, $\beta = 6.4$ case (which is a representative mesonic example). The plot shows the fits from all three methods above. This figure illustrates the points made above; the errors in the data for small times are clearly tiny.

We have argued that the absolute values of the $\chi^2/\text{d.o.f.}$ values might reasonably be expected to be large for the “Cont” and “2-exp” fits. However their *relative values* should correspond to the relative quality of fits of the two methods. From Tables 2,3,4 & 5 we see that the χ^2 for the “Cont” fit are smaller than (or, at worse, similar to) the “2-exp” fit in every case. In some cases (particularly for the Pseudoscalar meson) the χ^2 value for the “Cont” case is as much as an order of magnitude smaller than the “2-exp” case. This is again evidence that the “Cont”

fitting functions are an improvement over the traditional “2-exp” functions.

As examples of the quality of the fits, Figs. 2, 3 and 4 show the effective mass plots for the Clover, $\beta = 6.2$, Pseudoscalar case, the Wilson, $\beta = 6.4$, Vector meson case, and the Wilson, $\beta = 6.0$, nucleon case respectively. The central values of the effective mass from the three methods: “1-exp”; “Cont”; and “2-exp” are shown. (Note that the effective mass has been corrected for the effect of the backward moving state and should therefore be constant at large times approaching the middle of the lattice.) In these figures the “2-exp” fit can be seen to give a reasonable reproduction of the Monte Carlo data, however, the “Cont” method performs a little better. In particular the effect discussed in Sect. 4.1 at intermediate time values can be seen in the “2-exp” case. These three cases are a representative sample of all the cases studied, and support the conclusions above regarding the relative merits of the “2-exp” and “Cont” approaches.

Further evidence that the “Cont” method is an improvement over the “2-exp” case can be seen in Figs. 5 and 6. The channels shown are for the pseudoscalar and nucleon respectively for the Clover, $\beta = 6.0$ simulation. In these figures the mass, obtained from both the “Cont” and “2-exp” fits using $t = 2 \rightarrow t_{MAX}$, is plotted against t_{MAX} . (The “1-exp” fit using $t = 12 \rightarrow 28$ is shown as the solid horizontal line.) As can be seen from the fits, the “Cont” method converges much faster to the true mass value compared with the “2-exp” case. Other channels show a similar behaviour.

4.3 Parameters of the Excited State(s)

Clearly it is not sufficient for the “Cont” fits to reproduce the ground state parameters Z and M , and to have a sensible χ^2 , they must also give values for the continuum parameters, s_0 and ξ , which are acceptable within the assumptions of the QCDSR Continuum Model.

In Table 7 the values for s_0 (in GeV) are listed for all the cases studied. These values must satisfy two criteria: (i) since s_0 corresponds to a physical threshold, they should be constant (in GeV) for each channel as β is varied; and (ii) they should be large enough to be in a region where perturbation theory is valid. The second criterion is required so that the perturbative expression for the quark propagator, Eq. (12), is valid. From Table 7, it is clear that the s_0 values are roughly constant in β for the mesons, but not for the nucleon (particularly the Clover case). Also, for the pseudoscalar meson, the s_0 values are arguably too small ($\lesssim 2 GeV$) for perturbation theory to be considered reliable. Thus only the vector and axial mesons convincingly pass the criteria above.

We now turn to the values for ξ . Note that this parameter was introduced to parametrise the distortions introduced in the lattice formalism. It should therefore be unity in the continuum limit [1]. Table 8 displays the various values of ξ from the “Cont” fits. Clearly, in the case of the axial meson, the ξ values are not “ $\approx 1 + \mathcal{O}(a)$ ”. The large size of these ξ is because the leading term in the Continuum part of $G_2(t)$ for this channel is $\mathcal{O}(m_q^2)$ (see Eqs. (30) and (24)). This implies that ξ values several orders of magnitude larger than the other channels (which have $\mathcal{O}(1)$ terms in $G_2(t)$) are required.

In conclusion, the results of the continuum parameters, s_0 and ξ , cast doubt over the applicability of the “Cont” model, since the values obtained from the fits are not consistent with the assumptions made in the QCDSR Continuum Model.

Note, it is not possible to compare directly the values for ξ for Wilson, nucleon data with those in Ref. [1]. This is because the baryonic channels studied here have “thinned” correlation functions (see the discussion in Sect. 2). This affects the short-time region only, due to the presence of extra high energy states, and thus conceivably alters the values of ξ .

4.4 Discussion on the Fits

Summarising the subsections above, we see that the QCDSR Continuum Model fitting functions reproduce the correct ground state parameters, Z and M , of the Monte Carlo data in the meson case. The Continuum Model is not as successful however in the baryonic sector. The “2-*exp*” case does not appear to reproduce the ground state parameters as effectively as the “Cont” case for both baryons and mesons. We presented an explanation for this finding in Sect. 4.1. However, the values found for the continuum parameters s_0 and ξ cast doubt over the applicability of the “Cont” Ansatz, since the values obtained are not consistent with the assumptions used in its derivation. The conclusion therefore is to reject the QCDSR Continuum Model as a way of modelling these lattice correlation functions.

However it is clear that, apart from taking on non-physical values of its fitting parameters, the “Cont” Ansatz does fairly adequately reproduce the lattice correlation function data. Therefore we require similar fitting Ansätze as those in the “Cont” case, but without the corresponding restrictions on the parameters s_0 and ξ .

As we shall see in the next section, the naive non-relativistic quark model predicts essentially the same functional form for the hadronic correlators as in the QCDSR Continuum Model (for both the mesonic and baryonic cases). Therefore it is a

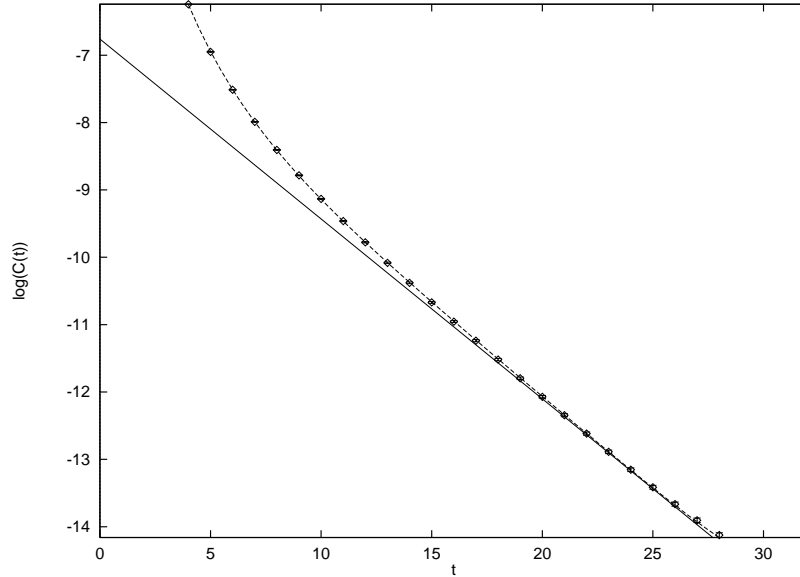


Fig. 1. *Plot of the (natural) logarithm of the correlation function for the $\beta = 6.4$, Wilson, Vector meson data. The curve is the result of the “Cont” fit and the straight line the result of the “1-exp” fit. The “2-exp” fit is indistinguishable from the “Cont” fit on this plot.*

candidate model to use to fit the data.

Before commencing the discussion on the quark model, we comment on the results of the Wilson and clover actions. It is natural to ask if we can observe any difference in the fitted parameters for these two actions which might be a signal for improvement. Studying the χ^2 values Tables 2, 3, 4 & 5 it is difficult to see discernible differences between the two actions.⁵ There are, however, clear differences between the Continuum parameters in the two actions, particularly for ξ (see Table 8). This is not surprising since differences between the two actions are known to occur at small times values (see [7]). However, the interpretation of these effects will require more work.

⁵ It is possible that there is some difference in the vector channel - see Table 4.

Nucleon				
Clover Action				
β		6.0	6.2	6.4
Z	1-exp	$[0.14 \pm 0.02] \times 10^{-5}$	$[0.14 \pm 0.05] \times 10^{-6}$	$[0.15 \pm 0.04] \times 10^{-7}$
	Cont	$[0.24 \pm 0.02] \times 10^{-5}$	$[0.30 \pm 0.03] \times 10^{-6}$	$[0.48 \pm 0.02] \times 10^{-7}$
	2-exp	$[0.34 \pm 0.04] \times 10^{-5}$	$[0.33 \pm 0.03] \times 10^{-6}$	$[0.50 \pm 0.02] \times 10^{-7}$
Ma	1-exp	0.828 ± 0.009	0.59 ± 0.02	0.438 ± 0.009
	Cont	0.865 ± 0.008	0.636 ± 0.009	0.491 ± 0.003
	2-exp	0.89 ± 0.01	0.643 ± 0.009	0.492 ± 0.003
χ^2	1-exp	$(1. \pm 1.)/15$	$(0.7 \pm 0.8)/9$	$(0.02 \pm 0.05)/3$
	Cont	$(1000. \pm 70.)/23$	$(310. \pm 60.)/22$	$(1000. \pm 60.)/21$
	2-exp	$(4000. \pm 100.)/23$	$(550. \pm 80.)/22$	$(1000. \pm 70.)/21$

Wilson Action				
β		6.0	6.1	6.4
Z	1-exp	$[0.16 \pm 0.02] \times 10^{-5}$	$[0.61 \pm 0.07] \times 10^{-6}$	$[0.23 \pm 0.04] \times 10^{-7}$
	Cont	$[0.24 \pm 0.02] \times 10^{-5}$	$[0.127 \pm 0.008] \times 10^{-5}$	$[0.92 \pm 0.05] \times 10^{-7}$
	2-exp	$[0.32 \pm 0.03] \times 10^{-5}$	$[0.144 \pm 0.009] \times 10^{-5}$	$[0.105 \pm 0.006] \times 10^{-6}$
Ma	1-exp	0.797 ± 0.008	0.737 ± 0.006	0.428 ± 0.006
	Cont	0.823 ± 0.007	0.776 ± 0.005	0.495 ± 0.004
	2-exp	0.845 ± 0.008	0.784 ± 0.005	0.503 ± 0.005
χ^2	1-exp	$(0.3 \pm 0.5)/15$	$(0.1 \pm 0.3)/11$	$(0.02 \pm 0.03)/3$
	Cont	$(220. \pm 40.)/23$	$(660. \pm 60.)/22$	$(2000. \pm 90.)/21$
	2-exp	$(1000. \pm 80.)/23$	$(1000. \pm 80.)/22$	$(2000. \pm 100.)/21$

Table 2

Values for the fitting parameters for the nucleon. The 1-exp, Cont and 2-exp refer to fits using Eqs. (32), (26) and (33) respectively.

Pseudoscalar Meson				
Clover Action				
β		6.0	6.2	6.4
Z	1-exp	0.0328 ± 0.0009	$[0.80 \pm 0.05] \times 10^{-2}$	$[0.27 \pm 0.01] \times 10^{-2}$
	Cont	0.0329 ± 0.0007	$[0.86 \pm 0.03] \times 10^{-2}$	$[0.278 \pm 0.009] \times 10^{-2}$
	2-exp	0.0349 ± 0.0007	$[0.92 \pm 0.03] \times 10^{-2}$	$[0.312 \pm 0.008] \times 10^{-2}$
Ma	1-exp	0.438 ± 0.001	0.294 ± 0.003	0.220 ± 0.001
	Cont	0.438 ± 0.001	0.296 ± 0.002	0.220 ± 0.001
	2-exp	0.441 ± 0.001	0.299 ± 0.002	0.224 ± 0.001
χ^2	1-exp	$(0.2 \pm 0.3)/15$	$(0.01 \pm 0.05)/9$	$(0.001 \pm 0.003)/3$
	Cont	$(3. \pm 1.)/23$	$(3. \pm 2.)/22$	$(1.1 \pm 0.5)/21$
	2-exp	$(48. \pm 5.)/23$	$(18. \pm 4.)/22$	$(21. \pm 4.)/21$

Wilson Action				
β		6.0	6.1	6.4
Z	1-exp	0.0244 ± 0.0007	0.0149 ± 0.0005	$[0.210 \pm 0.009] \times 10^{-2}$
	Cont	0.0226 ± 0.0007	0.0144 ± 0.0004	$[0.200 \pm 0.009] \times 10^{-2}$
	2-exp	0.0253 ± 0.0006	0.0155 ± 0.0004	$[0.236 \pm 0.005] \times 10^{-2}$
Ma	1-exp	0.423 ± 0.001	0.404 ± 0.001	0.205 ± 0.001
	Cont	0.420 ± 0.001	0.403 ± 0.001	0.204 ± 0.002
	2-exp	0.425 ± 0.001	0.406 ± 0.001	0.210 ± 0.001
χ^2	1-exp	$(0.3 \pm 0.4)/15$	$(0.1 \pm 0.2)/11$	$(0.002 \pm 0.004)/3$
	Cont	$(20. \pm 4.)/23$	$(1. \pm 1.)/22$	$(0.4 \pm 0.6)/21$
	2-exp	$(23. \pm 4.)/23$	$(18. \pm 5.)/22$	$(27. \pm 5.)/21$

Table 3

Values for the fitting parameters for the pseudoscalar meson. The 1-exp, Cont and 2-exp refer to fits using Eqs. (32), (28) and (33) respectively.

Vector Meson (Spatial Components)				
Clover Action				
β		6.0	6.2	6.4
Z	1-exp	$[0.93 \pm 0.06] \times 10^{-2}$	$[0.18 \pm 0.03] \times 10^{-2}$	$[0.51 \pm 0.04] \times 10^{-3}$
	Cont	0.0106 ± 0.0003	$[0.27 \pm 0.01] \times 10^{-2}$	$[0.77 \pm 0.03] \times 10^{-3}$
	2-exp	0.0121 ± 0.0004	$[0.300 \pm 0.010] \times 10^{-2}$	$[0.94 \pm 0.03] \times 10^{-3}$
Ma	1-exp	0.548 ± 0.004	0.378 ± 0.006	0.285 ± 0.003
	Cont	0.556 ± 0.003	0.397 ± 0.003	0.300 ± 0.002
	2-exp	0.565 ± 0.003	0.403 ± 0.003	0.309 ± 0.002
χ^2	1-exp	$(1. \pm 1.)/15$	$(0.4 \pm 0.6)/9$	$(0.02 \pm 0.02)/3$
	Cont	$(130. \pm 30.)/23$	$(120. \pm 20.)/22$	$(91. \pm 2.)/21$
	2-exp	$(610. \pm 60.)/23$	$(270. \pm 40.)/22$	$(290. \pm 30.)/21$

Wilson Action				
β		6.0	6.1	6.4
Z	1-exp	0.0102 ± 0.0004	$[0.57 \pm 0.03] \times 10^{-2}$	$[0.62 \pm 0.04] \times 10^{-3}$
	Cont	$[0.95 \pm 0.03] \times 10^{-2}$	$[0.59 \pm 0.02] \times 10^{-2}$	$[0.74 \pm 0.03] \times 10^{-3}$
	2-exp	0.0120 ± 0.0003	$[0.68 \pm 0.02] \times 10^{-2}$	$[0.99 \pm 0.03] \times 10^{-3}$
Ma	1-exp	0.508 ± 0.003	0.466 ± 0.002	0.267 ± 0.003
	Cont	0.505 ± 0.002	0.468 ± 0.002	0.274 ± 0.002
	2-exp	0.517 ± 0.002	0.474 ± 0.002	0.286 ± 0.002
χ^2	1-exp	$(0.3 \pm 0.6)/15$	$(0.4 \pm 0.6)/11$	$(0.008 \pm 0.009)/3$
	Cont	$(20. \pm 5.)/23$	$(8. \pm 5.)/22$	$(11. \pm 4.)/21$
	2-exp	$(200. \pm 20.)/23$	$(110. \pm 20.)/22$	$(180. \pm 20.)/21$

Table 4

Values for the fitting parameters for the (spatial components of the) vector meson. The 1-exp, Cont and 2-exp refer to fits using Eqs. (32), (29) and (33) respectively.

Axial-Vector Meson (Temporal Components)				
Clover Action				
β		6.0	6.2	6.4
Z	1-exp	$[0.171 \pm 0.008] \times 10^{-2}$	$[0.37 \pm 0.03] \times 10^{-3}$	$[0.111 \pm 0.009] \times 10^{-3}$
	Cont	$[0.179 \pm 0.006] \times 10^{-2}$	$[0.38 \pm 0.02] \times 10^{-3}$	$[0.118 \pm 0.004] \times 10^{-3}$
	2-exp	$[0.180 \pm 0.006] \times 10^{-2}$	$[0.38 \pm 0.02] \times 10^{-3}$	$[0.118 \pm 0.004] \times 10^{-3}$
Ma	1-exp	0.437 ± 0.002	0.293 ± 0.004	0.217 ± 0.003
	Cont	0.440 ± 0.002	0.295 ± 0.004	0.219 ± 0.002
	2-exp	0.440 ± 0.002	0.295 ± 0.004	0.219 ± 0.002
χ^2	1-exp	$(0.3 \pm 0.2)/15$	$(0.06 \pm 0.06)/9$	$(0.02 \pm 0.02)/3$
	Cont	$(10. \pm 3.)/23$	$(1.2 \pm 0.8)/22$	$(2. \pm 1.)/21$
	2-exp	$(15. \pm 4.)/23$	$(1.5 \pm 0.9)/22$	$(2. \pm 1.)/21$

Wilson Action				
β		6.0	6.1	6.4
Z	1-exp	$[0.23 \pm 0.01] \times 10^{-2}$	$[0.159 \pm 0.006] \times 10^{-2}$	$[0.126 \pm 0.009] \times 10^{-3}$
	Cont	$[0.234 \pm 0.007] \times 10^{-2}$	$[0.170 \pm 0.004] \times 10^{-2}$	$[0.140 \pm 0.005] \times 10^{-3}$
	2-exp	$[0.236 \pm 0.006] \times 10^{-2}$	$[0.171 \pm 0.004] \times 10^{-2}$	$[0.140 \pm 0.005] \times 10^{-3}$
Ma	1-exp	0.422 ± 0.002	0.403 ± 0.002	0.201 ± 0.002
	Cont	0.423 ± 0.002	0.406 ± 0.002	0.205 ± 0.001
	2-exp	0.423 ± 0.002	0.406 ± 0.002	0.205 ± 0.001
χ^2	1-exp	$(0.5 \pm 0.5)/15$	$(0.8 \pm 0.5)/11$	$(0.01 \pm 0.01)/3$
	Cont	$(2. \pm 2.)/23$	$(5. \pm 3.)/22$	$(0.8 \pm 0.9)/21$
	2-exp	$(4. \pm 2.)/23$	$(6. \pm 3.)/22$	$(0.9 \pm 1.0)/21$

Table 5

Values for the fitting parameters for the (temporal components of the) axial meson. The 1-exp, Cont and 2-exp refer to fits using Eqs. (32), (30) and (33) respectively.

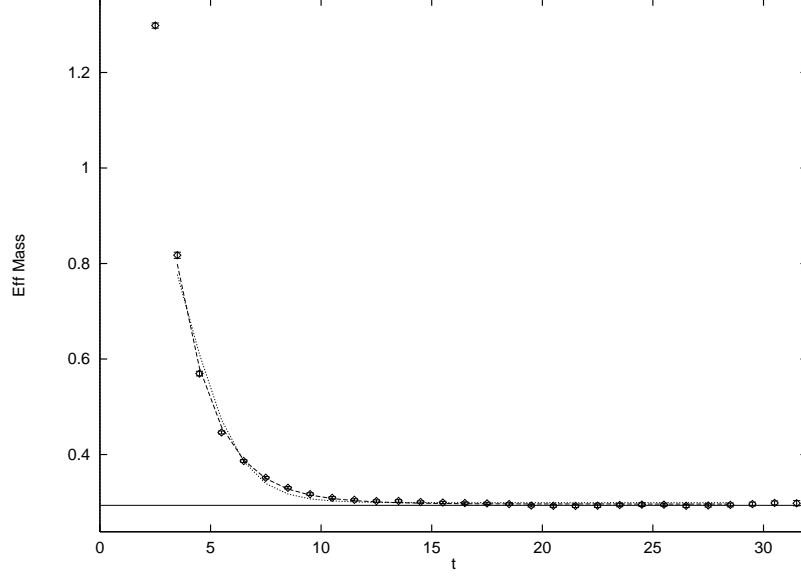


Fig. 2. *Effective mass plot for the $\beta = 6.2$, Clover, Pseudoscalar data. The values of M from the fits to the “1-exp” is shown by a horizontal solid line. The “Cont” is the dashed curve, and the “2-exp” is the dotted curve.*

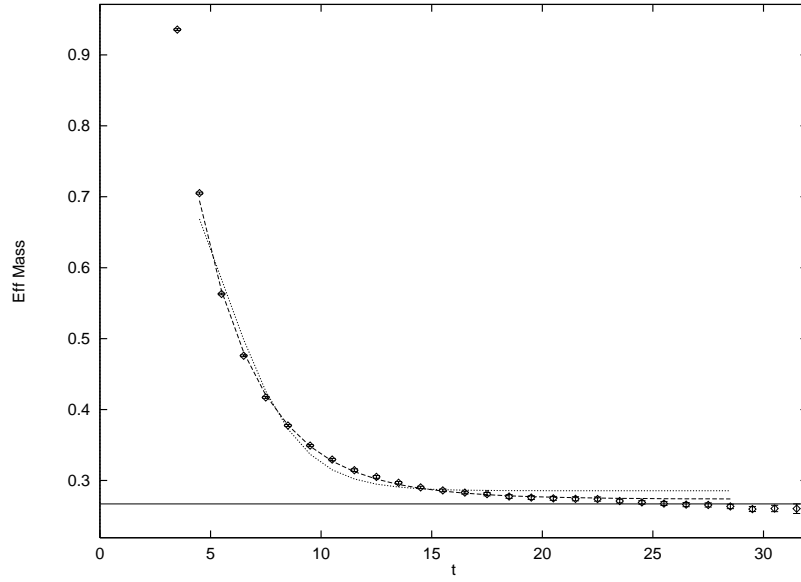


Fig. 3. *Effective mass plot for the $\beta = 6.4$, Wilson, Vector meson data. The values of M from the fits to the “1-exp” is shown by a horizontal solid line. The “Cont” is the dashed curve, and the “2-exp” is the dotted curve.*

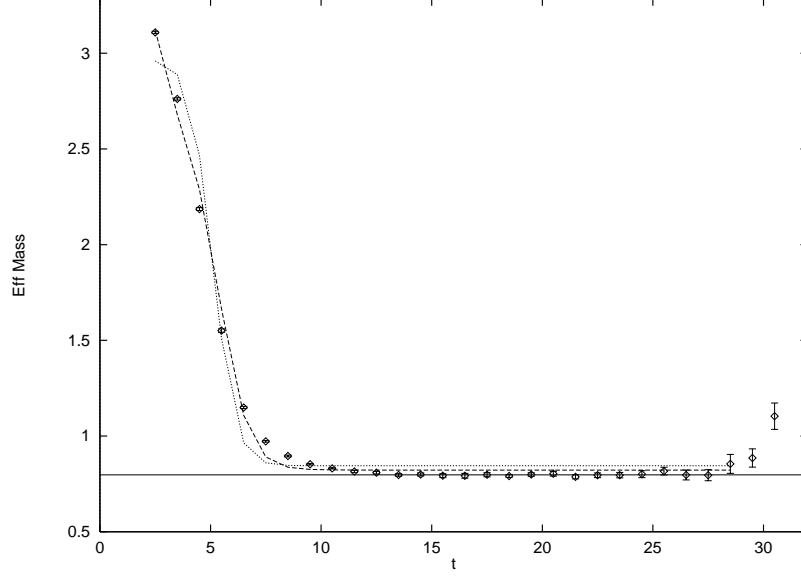


Fig. 4. *Effective mass plot for the $\beta = 6.0$, Wilson, Nucleon data. The values of M from the fits to the “1-exp” is shown by a horizontal solid line. The “Cont” is the dashed curve, and the “2-exp” is the dotted curve.*

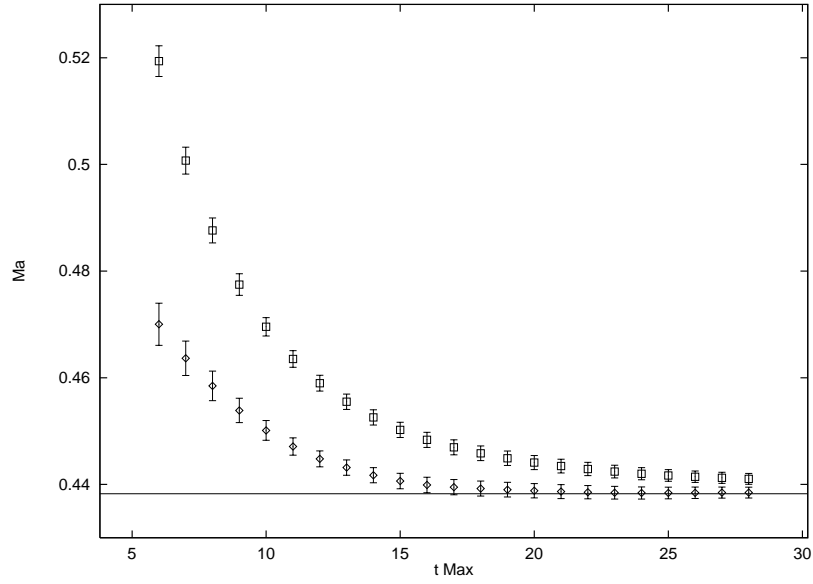


Fig. 5. *Results for the mass from the fit to the $\beta = 6.0$, Clover, pseudoscalar case for times $t = 2 \rightarrow t_{MAX}$. The “Cont” fit results are shown as diamonds, and the “2-exp” case as squares. The “1-exp” fit for $t = 12 \rightarrow 28$ is depicted by a horizontal solid line.*

Clover Action			
β	6.0	6.2	6.4
1-exp	12-28	18-28	24-28
Cont	2-28	3-28	4-28
2-exp	2-28	3-28	4-28

Wilson Action			
β	6.0	6.1	6.4
1-exp	12-28	16-28	24-28
Cont	2-28	3-28	4-28
2-exp	2-28	3-28	4-28

Table 6
The time windows used in each of the fitting methods.

5 Quark Models

5.1 Non-relativistic Quark Model

The quark model has had considerable success in reproducing many of the features of the hadronic spectrum [18]. It is thus natural to check its predictions for the hadronic correlators with the lattice Monte Carlo data. We present firstly the derivation of the hadronic correlators for the non-relativistic quark model, and then the relativistic case.

The aim of this exercise is to determine the density of states function $\rho(s)$ which defines the number of states per unit energy range. Taking the quarks as on-shell, there are 3 degrees of freedom available for each quark in the hadron: one

s_0 [GeV]			
Clover Action			
β	6.0	6.2	6.4
Nucleon	5.8 ± 0.2	8.5 ± 0.8	10.1 ± 0.5
Pseudoscalar Meson	1.87 ± 0.06	2.0 ± 0.2	1.6 ± 0.1
Vector Meson	2.57 ± 0.09	2.9 ± 0.2	2.4 ± 0.1
(Spatial Components)			
Axial-Vector Meson	4.1 ± 0.2	5.0 ± 0.4	5.3 ± 0.5
(Temporal Components)			
Wilson Action			
β	6.0	6.1	6.4
Nucleon	5.0 ± 0.1	5.9 ± 0.4	6.9 ± 0.3
Pseudoscalar Meson	1.34 ± 0.05	1.7 ± 0.1	1.4 ± 0.1
Vector Meson	1.77 ± 0.04	2.0 ± 0.1	1.97 ± 0.08
(Spatial Components)			
Axial-Vector Meson	3.5 ± 0.1	3.5 ± 0.3	4.2 ± 0.5
(Temporal Components)			

Table 7
Values for the fitting parameter s_0 in GeV from the “Cont” fit.

ξ			
Clover Action			
β	6.0	6.2	6.4
Nucleon	72.4 ± 0.5	49.7 ± 0.6	22.6 ± 0.4
Pseudoscalar Meson	9.49 ± 0.07	6.8 ± 0.1	4.87 ± 0.07
Vector Meson	9.41 ± 0.07	5.70 ± 0.10	2.85 ± 0.04
(Spatial Components)			
Axial-Vector Meson	$[1.54 \pm 0.06] \times 10^3$	$[1.3 \pm 0.2] \times 10^3$	$[6. \pm 2.] \times 10^2$
(Temporal Components)			
Wilson Action			
β	6.0	6.1	6.4
Nucleon	6.73 ± 0.03	5.58 ± 0.06	1.82 ± 0.04
Pseudoscalar Meson	3.82 ± 0.01	4.03 ± 0.06	3.74 ± 0.04
Vector Meson	3.40 ± 0.02	3.28 ± 0.04	2.66 ± 0.02
(Spatial Components)			
Axial-Vector Meson	$126. \pm 8.$	$56. \pm 2.$	$94. \pm 8.$
(Temporal Components)			

Table 8
Values for the fitting parameter ξ from the “Cont” fit.

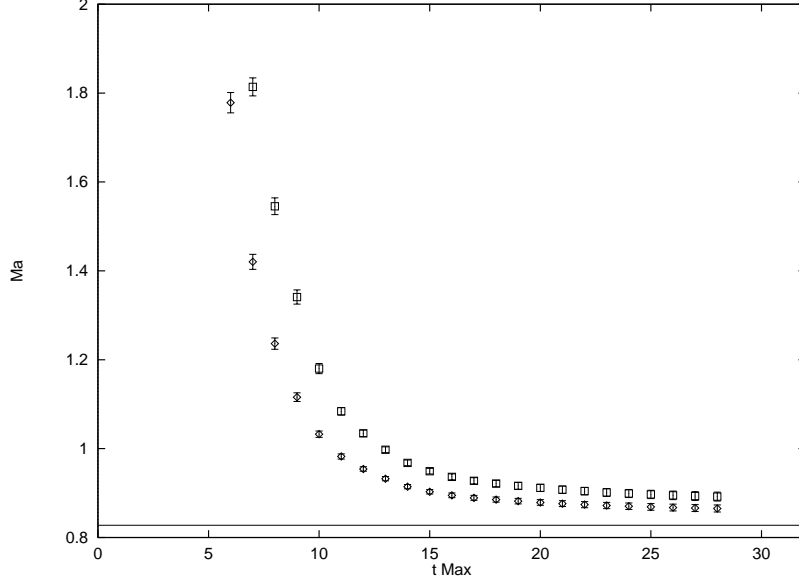


Fig. 6. *As in Figure 5, but for the Nucleon case.*

per spatial momentum component. Therefore in the case of mesons there are naively 6 degrees of freedom, with 9 degrees of freedom for baryons. However, there are 4 constraint equations. Three correspond to demanding that the total 3-momentum is fixed to the hadron's momentum (which is zero in the correlators we are studying), and one which corresponds to demanding that the total kinetic energy is fixed to s . This leaves 2 degrees of freedom for the mesons and 5 degrees of freedom for the baryons. This simple, non-relativistic analysis leads to the following form for the spectral density.

$$\text{For mesons: } \rho_{nrqm}(s) \sim s^2 \quad (34)$$

$$\text{For baryons: } \rho_{nrqm}(s) \sim s^5 \quad (35)$$

The above continuum-like behaviour for $\rho(s)$ is clearly most appropriate for large s where the quarks are approximately free. Therefore the actual density of states can be approximated by

$$\rho(s) = \frac{Z}{2M} \delta(s - M) + \theta(s - s_0) \rho_{nrqm}(s), \quad (36)$$

where the delta-function represents the ground state, and the non-relativistic quark model result is used for the continuum (beginning at the threshold energy s_0). Using this definition of $\rho(s)$ in the spectral equation (Eq. (14)) we obtain

for mesons:

$$G_2(t) = \frac{Z}{2M} e^{-Mt} + K \left(\frac{1}{t^3} + \frac{s_0}{t^2} + \frac{s_0^2}{2t} \right) e^{-s_0 t}, \quad (37)$$

and for baryons:

$$G_2(t) = \frac{Z}{2M} e^{-Mt} + K' \left(\frac{1}{t^6} + \frac{s_0}{t^5} + \frac{s_0^2}{2t^4} + \frac{s_0^3}{3!t^3} + \frac{s_0^4}{4!t^2} + \frac{s_0^5}{5!t} \right) e^{-s_0 t}, \quad (38)$$

where K and K' are some numerical constants. Note that Eqs. (37&38) are identical to Eqs. (26-31) in Sect. 3 with $m_q = 0$. Since numerically the terms $\mathcal{O}(m_q)$ and $\mathcal{O}(m_q^2)$ are insignificant, we have shown that the non-relativistic quark model predicts essentially the same functional form as the QCD Sum Rules Continuum Model for these channels.

Thus we have achieved the aim raised in Sect. 4.4: we have found an Ansatz which reproduces the data better than the “2-exp” fits, but which doesn’t suffer from the unphysical parameter values of the “Cont” fit.

5.2 Relativistic Quark Model

We now turn our attention to the derivation of $\rho(s)$ in the relativistic quark model. In this case we can represent the number of states as:

$$\text{Number of states} \sim \int \frac{d^3 p_1}{2E_1} \int \frac{d^3 p_2}{2E_2} \delta^3(\vec{p}_1 + \vec{p}_2) \delta((p_1^{(0)})^2 + (p_2^{(0)})^2 - s^2), \quad (39)$$

in the meson case, with an obvious generalisation for baryons. The main difference between this case and the non-relativistic case is the energy factors in the denominators of the normalisation. Thus we obtain two powers of s less in the meson case, and 3 powers of s less in the baryonic case. i.e.

$$\text{For mesons: } \rho_{rqm}(s) \sim s^0 \quad (40)$$

$$\text{For baryons: } \rho_{rqm}(s) \sim s^2 \quad (41)$$

Following the above analysis, the 2-point hadronic correlators can easily be derived;

for mesons:

$$G_2(t) = \frac{Z}{2M} e^{-Mt} + K \left(\frac{1}{t} \right) e^{-s_0 t} \quad (42)$$

and for baryons:

$$G_2(t) = \frac{Z}{2M} e^{-Mt} + K' \left(\frac{1}{t^3} + \frac{s_0}{t^2} + \frac{s_0^2}{2t} \right) e^{-s_0 t}. \quad (43)$$

Note that the relativistic quark model prediction for $G_2(t)$ for baryons is identical to the non-relativistic mesonic $G_2(t)$.

5.3 Quark Model Fits

It is natural to wonder if there is any way of using the lattice correlation function data to pin down the best form of the density of states $\rho(s)$. With this in mind we assume that the density of states has the following form:

$$\rho(s) = \frac{Z}{2M} \delta(s - M) + \theta(s - s_0) K s^n \quad (44)$$

where n is to be determined from the fit. The two-point correlation function for this Ansatz is defined, as usual, from eq.(14). Eq. (44) has both the non-relativistic and relativistic forms as special cases. Fig. 7 shows the χ^2 value plotted against n for fits to the 6 sets of pseudoscalar data in table 1 using eq.(44). As can be seen from the plot, there is a distinct minimum at $n = 2$ for five of the six data sets. This confirms the non-relativistic quark model Ansatz (i.e. $n = 2$) as the preferred choice for this channel. The vector meson case is plotted in Fig. 8. Here, as expected, the signal is worse,⁶ but the minimum is certainly not far off $n = 2$. When these fits are applied to the nucleon, the data is more poorly behaved again (see Fig. 9). However, it is clear that the minimum has shifted significantly to larger n values compared with the mesonic cases - it is now roughly between $n = 5$ and $n = 10$.

We now study the behaviour of the Ansatz eq.(44) as a function of quark mass. In Fig. 10 the χ^2 values for the pseudoscalar fits as a function of n are plotted for lighter quarks, corresponding to $M_V \approx 900 MeV$. (Recall that all other data in this work is for quark masses corresponding to $M_V \approx 1.1 GeV$ - see Table

⁶In general, the pseudoscalar channel has the best signal to noise ratio.

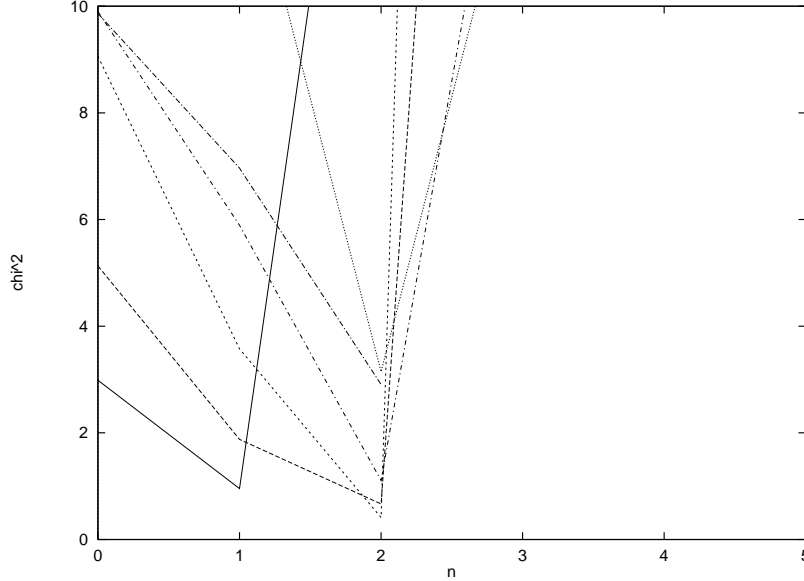


Fig. 7. The χ^2 value plotted against n for the pseudoscalar meson case for the fit corresponding to eq.(44). The six lines are drawn as a guide for the eye only. They join points from the same simulations (see Table 1).

1.) Comparing Fig. 10 with Fig. 7 one can see a tendency for the minimum χ^2 to decrease from $n = 2$ as the quark mass decreases. This fits nicely with our intuition - lighter quarks should eventually become relativistic which corresponds to $n = 0$ (see Sec. 5.2).

6 Discussion & Conclusion

We have begun this work with a comprehensive study of the QCD Sum Rule Continuum Model as applied to lattice two-point correlation functions using the method first introduced by Leinweber [1,2]. We have extended his work by including mesonic states, by fitting lattice data at several lattice spacings and by using two formulations of the lattice action. We have found that the QCD Sum Rule Continuum Model successfully fits the lattice data, and the quality of the fits is a significant improvement over the conventional “2-exponential” fits. However, while the results of the fits are successful, the values of the parameters in the fits are unphysical. This leads us to the conclusion (somewhat contrary to that of [1]) that this model cannot self-consistently fit lattice data.

We have then searched for a model that reproduces a similar functional form as

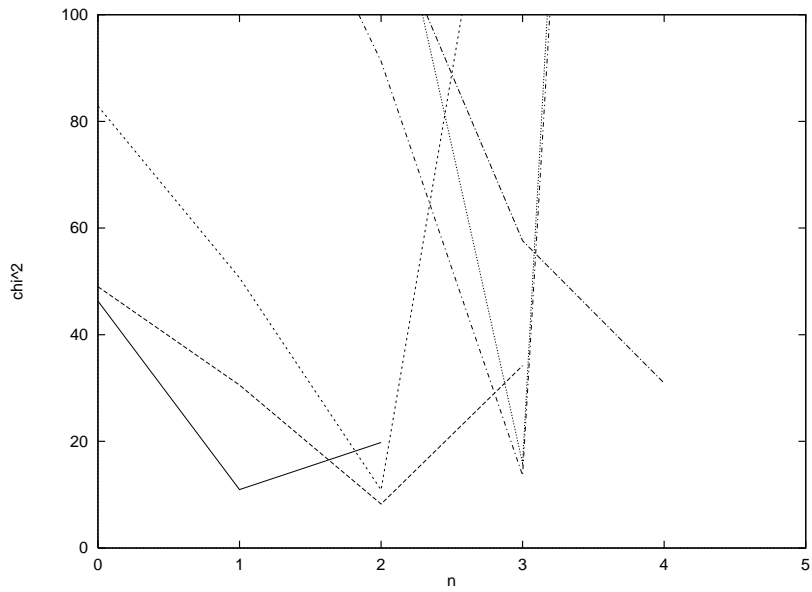


Fig. 8. As in Fig. 7 but for the vector meson case. No points are plotted in cases where the fits did not converge.

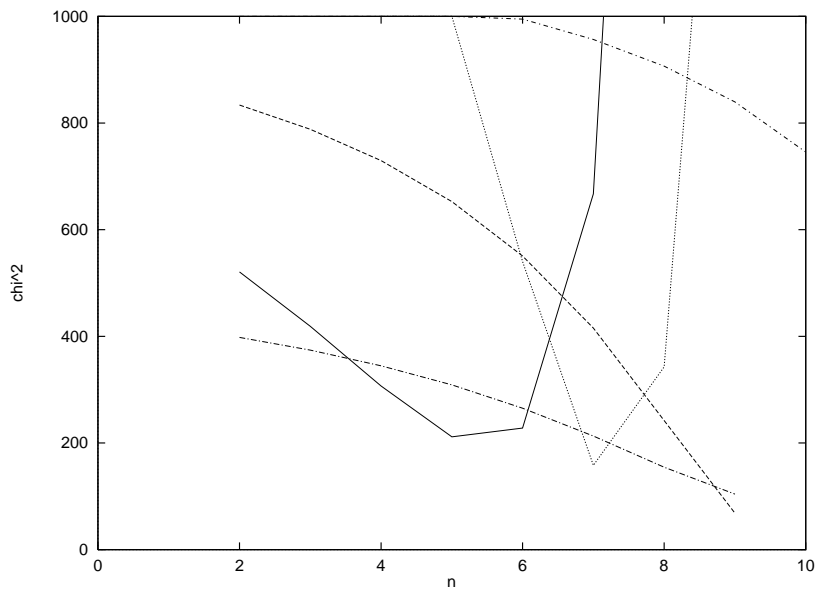


Fig. 9. As in Fig. 7 but for the nucleon case. No points are plotted in cases where the fits did not converge.

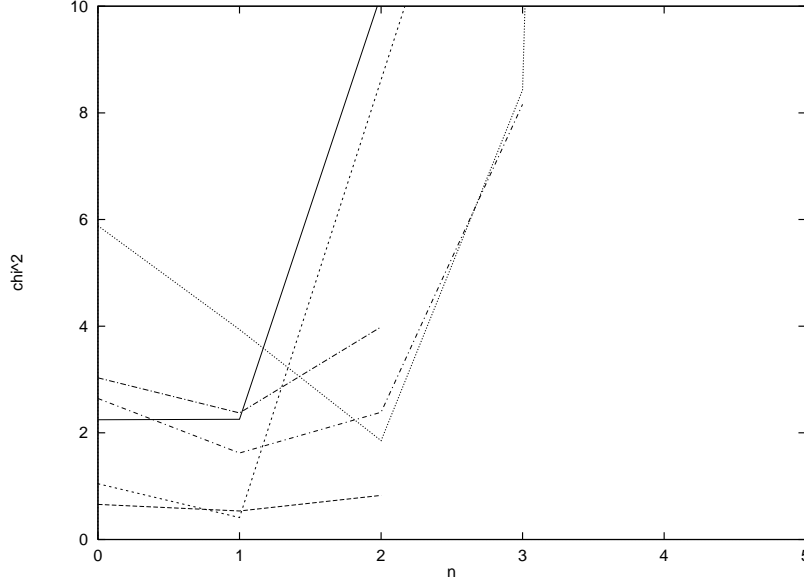


Fig. 10. *As in Fig. 7 but for lighter quark masses corresponding to $M_V \approx 900\text{MeV}$. No points are plotted in cases where the fits did not converge.*

the QCD Continuum Model, but which does not have the same restrictions on its parameters. Both the non-relativistic and relativistic quark models were studied. By using a fitting function which interpolated between the two, it was found that the non-relativistic quark model was qualitatively better than its relativistic counterpart for the quark mass studied. In the case of the pseudoscalar meson, these remarks are more quantitative. In addition, by studying lighter quark masses, the best fitting function was found to tend towards the relativistic form, as expected.

Thus we have found a model which appears to correctly parametrise the rôle of the excited states. The functions that we have found can be widely used for Lattice Gauge Theories fits when the time separation in the correlation functions is forced to be small. In particular, it would be interesting to apply these functions to the case of the static case of the Heavy Quark Effective Theory on the lattice where ground state properties are poorly isolated (see, for example, [19]) and in glueball studies.

Acknowledgement

We wish to thank the APE collaboration for allowing us to use the lattice correlation function data presented here. We also thank Ian Drummond, Simon Hands,

Derek Leinweber, Vittorio Lubicz, Martin Lüscher, Graham Shore and John Stack for useful discussions. CRA would like to acknowledge help from John Evans.

S. C. thanks the Organising Committee for his participation at the 16th UK Institute at Swansea, where part of this work was carried out.

This work was supported by the EC Contract “Computational Particle Physics” CHRX-CT92-0051, and by the EC Human Capital and Mobility Program, contracts ERBCHBICT941462 and ERBCHBGCT940665 and by a grant from the Nuffield Foundation.

References

- [1] D.B.Leinweber, Phys. Rev. **D51** (1995) 6369
- [2] D.B.Leinweber, Phys. Rev. **D51** (1995) 6383
- [3] M.A. Shifman, A.I. Vainshtein and V.I. Zakharov, Nucl. Phys. **B 147** (1979) 385, 448
- [4] K.G.Wilson, Phys. Rev. **D10** (1974) 2445, and in “New Phenomena in Subnuclear Physics”, Plenum Press, New York (1977) (A.Zichichi ed.)
- [5] B.Sheikholeslami and R.Wohlert, Nucl.Phys. **B259** (1985) 572.
- [6] M.-C. Chu, J. M. Grandy, S. Huang and J. W. Negele, Phys. Rev. **D48** (1993) 3340.
- [7] S.J.Hands, P.W.Stephenson and A.McKerrell (The UKQCD Collaboration), Phys. Rev. **D51** (1995) 6394
- [8] E. Shuryak, Rev. Mod. Phys. **65** (1993) 1.
- [9] C.R. Allton and S. Capitani, hep-lat/9709046, *to be published in* Nucl. Phys. **B (Proc. Suppl.)**.
- [10] APE Collaboration, C.R. Allton et al, Phys. Lett. **B 326** (1994) 295
- [11] APE Collaboration, C.R.Allton et al, Nucl. Phys. **B (Proc. Suppl.) 42** (1995) 385, and *in preparation*
- [12] M. Crisafulli et al, Phys. Lett. **B 369** (1996) 325.
- [13] C.R. Allton, V. Giménez, L. Giusti and F. Rapuano, Nucl. Phys. **B489** (1997) 427.
- [14] UKQCD Collaboration, C.R.Allton et al, Phys. Rev. **D 49** (1994) 474
- [15] B. L. Ioffe, Nucl. Phys. **B188** (1981) 317.

- [16] APE Collaboration (P. Bacilieri et al.), Nucl. Phys. **B 317** (1989) 509.
- [17] JLQCD Collaboration (S. Aoki et al.), Nucl. Phys. **B (Proc. Suppl.) 47** (1996) 354.
- [18] *Current Physics Studies and Comments*, vol. 9, Quarkonia (ed. W. Buchmüller) North Holland, 1992.
- [19] E. Eichten, Nucl. Phys. **B (Proc. Suppl.) 20** (1991) 475, C. W. Bernard, Nucl. Phys. **B (Proc. Suppl.) 34** (1994) 47, C. R. Allton, Nucl. Phys. **B (Proc. Suppl.) 47** (1996) 31.